JOURNAL OF GEOPHYSICAL RESEARCH, VOL. 92, NO. C4, PAGES 3905–3912, APRIL 15, 1987

# Wave Refraction by a Current Whirl

MARTIN MATHIESEN

*Norwegian Hydrotechnical Laboratory, Trondheim*

A computer model for the computation of refraction of ocean directional wave spectra has been developed. The model is applied to wave propagation through a circular current whirl. Both refraction diagrams and computed directional wave spectra are presented. Wave heights are computed for points outside the whirl. Relative changes in wave heights are found to be within ±20%. The computations reveal two areas of crossing seas on the lee side of the whirl. Between these areas is an area of reduced wave heights and nearly unidirectional waves.

## INTRODUCTION

The theory of wave refraction was extended to directional wave spectra by *Longuet-Higgins* [1957], who showed that the spectral wave energy density is conserved along a ray. His theoretical results were translated into practical use by *Abernethy and Gilbert* [1975], who presented a computer method for the calculation of refraction of wave spectra. This method uses the so-called backward ray tracing technique, whereby the directional wave spectrum at an inshore point of interest is determined in terms of an offshore directional wave spectrum model. Since the ocean wave field can be given a realistic representation through the use of directional wave spectra, reliable estimates of wave heights are obtained.

The theory of refraction of ocean waves referred to above is concerned only with refraction due to the varying depth. When considering both depth and current refraction, the spectral density is no longer conserved. The basic result then is that the spectral wave action density is conserved along a ray, as follows from the work of *Bretherton and Garrett* [1968]. The use of backward ray tracing methods in the analysis of depth and current refraction at first received little attention except for *Tayfun et al.* [1976], who presented results from unidirectional shear current models for which ray data were obtained analytically.

Numerical methods for the computation of depth and current refraction of directional wave spectra were presented first by *Brink-Kjær* [1984] and *Mathiesen* [1984] and later by Treloar [1986]. These methods differ only by the choice of solution technique used for the determination of ray paths: the rays are computed either through direct numerical integration of the ray equations or through the computation of ray curvature.

In this study we are concerned with the effects of wave refraction by a current whirl typical of the whirls appearing in the Norwegian coastal current. By using the backward ray tracing technique, we show how the directional wave spectrum varies over a large area on the lee side of the whirl. The study extends the work of *Mapp et al.* [1985], who used the forward ray tracing technique to study wave refraction by warm core rings, similar in form to the present current whirl model.

The spectral computations performed are limited to points outside the current whirl. This means that the wave data presented are fairly independent of wave height but are dependent on the direction of the incoming waves. As regards the navigational conditions for passing ships, we believe that wave form is just as important as wave height. The emphasis in the presentation is therefore as much on changes in the directional distribution of the waves as on changes in wave height.

In the following we first give a brief introduction to the theory of wave refraction and a presentation of the numerical method used in the wave computations. We then describe the current whirl model and the input "offshore" wave spectrum model. Finally, we present the results from the wave refraction computations and discuss the possible extension of the applicability of the computer model.



Paper number 6C0741.
0148-0227/87/006C-0741$05.00

## WAVE REFRACTION

We start by giving a brief introduction to the theory of wave propagation of ocean surface waves in an area of varying depths and varying currents. For a more detailed presentation, we refer to *Phillips* [1977, pp. 23–35, 59–60, 179–183].

We assume that the waves can be described within the framework of linear wave theory, that is,

$$ak \ll 1$$

$$a/h \ll (kh)^2$$

when $kh \ll 1$, where $a$ is the wave amplitude, $k = |\mathbf{k}|$ is the wave number, and $h$ is the water depth. The wavelength is defined by $L = 2\pi/k$. We further assume that the relative change in water depth over wavelength is small:

$$|\nabla h|/kh \ll 1$$

and that the relative change in the current velocity $\mathbf{u}$ over wavelength and period is small;

$$|\nabla \mathbf{u}|/ku \ll 1 \qquad |\partial \mathbf{u}/\partial t|/\omega u \ll 1$$

where $\omega$ is the absolute angular wave frequency. The wave period is defined by $T = 2\pi/\omega$.

The results obtained are the ray equations

$$d\mathbf{r}/dt = \mathbf{c}_g + \mathbf{u} \tag{1}$$

$$d\omega/dt = \mathbf{k} \cdot (\partial \mathbf{u}/\partial t) \tag{2}$$

$$d\mathbf{k}/dt = -(\partial\sigma/\partial h)\nabla h - (\nabla \mathbf{u}) \cdot \mathbf{k} \tag{3}$$

$$d(S(\mathbf{k})/\sigma)/dt = 0 \tag{4}$$

where the rays $\mathbf{r} = \mathbf{r}(t)$ are parametric curves which can conveniently be interpreted as streamlines of wave energy trans-

port. The other variables are the relative group velocity $\mathbf{c}_g$, the intrinsic angular frequency $\sigma$, and the wave number spectrum $S(\mathbf{k})$.

The ray equations have to be solved together with the Doppler shift equation

$$\omega = \sigma + \mathbf{k} \cdot \mathbf{u} \tag{5}$$

and the dispersion relation

$$\sigma^2 = gk \tanh (kh) \tag{6}$$

where $g$ is the acceleration due to gravity.

By tracing the rays backward from points in the inshore area outward to the offshore area where the waves do not refract, we see from (4) that the inshore spectrum $S$ can be determined in terms of any choice of offshore spectrum model $S_0$ by

$$S(\mathbf{k}) = (\sigma/\sigma_0)S_0(\mathbf{k}_0) \tag{7}$$

where the zero index refers to offshore values.

When the current field is assumed steady in time, we see from (2) that the absolute frequency $f = \omega/2\pi$ is constant along a ray. It is then convenient to use the directional wave spectrum $S(f, \theta)$ obtained from $S(\mathbf{k})$ through the relation

$$S(\mathbf{k}) = J(f, \theta)S(f, \theta) \tag{8}$$

where $\theta$ is the wave direction and $J(f, \theta)$ is the Jacobian determinant of the mapping from wave number to frequency direction domain. The Jacobian is given by

$$J(f, \theta) = |\partial\omega/\partial\mathbf{k} \times \partial\theta/\partial\mathbf{k}|/2\pi$$

which after insertion for the partial derivatives may be rewritten in the form

$$J(f, \theta) = \mathbf{c}_g \cdot (\mathbf{c}_g + \mathbf{u})/2\pi k c_g \tag{9}$$

Consequently, we can write

$$S(f, \theta) = T(f, \theta, \theta_0(f, \theta))S_0(f, \theta_0(f, \theta)) \tag{10}$$

where the transfer function $T$ is defined by

$$T(f, \theta, \theta_0) = J_0(f, \theta_0)\sigma/J(f, \theta)\sigma_0 \tag{11}$$

We note that in spectral refraction studies the only purpose of the ray calculations is to establish the relation $\theta_0 = \theta_0(f, \theta)$ between the inshore and the offshore wave directions. Backward ray tracing poses no new computational problems, as the computations can be performed in a "forward mode" simply by reversing the current field prior to computations.

## Numerical Method

A ray is a parametric curve in the plane and is therefore uniquely determined by its curvature. This means that the ray paths can be obtained numerically through the calculation of ray curvature. The ray curvature $\kappa$ is computed from

$$\kappa = (d\mathbf{r}/dt \times d^2\mathbf{r}/dt^2)_z/|d\mathbf{r}/dt|^3 \tag{12}$$

where the subscript $z$ denotes the vertical component of the vector.

Noting that $\mathbf{c}_g = k^{-1}(\partial\sigma/\partial k)\mathbf{k}$, $\sigma = \sigma[k(\mathbf{k}(t)), h(\mathbf{r}(t))]$ and $\mathbf{u} = \mathbf{u}(\mathbf{r}(t))$, the vector $d^2\mathbf{r}/dt^2$ is derived from (1) using the chain rule for differentiation. The result obtained is

$$\begin{aligned} d^2\mathbf{r}/dt^2 &= (d\mathbf{r}/dt) \cdot \nabla\mathbf{u} + k^{-2}\{[\partial^2\sigma/\partial k^2 - k^{-1}\partial\sigma/\partial k][\mathbf{k} \cdot (d\mathbf{k}/dt)] \\ &\quad + k[\partial^2\sigma/\partial k\partial h][(d\mathbf{r}/dt) \cdot \nabla h]\}\mathbf{k} + k^{-1}(\partial\sigma/\partial k)(d\mathbf{k}/dt) \end{aligned} \tag{13}$$

Since the curvature is slowly varying along the ray, points along the ray path can be determined by assuming that the curvature is locally constant. In this way the rays are modeled as a progression of circular arcs.

In order to update the ray curvature for continued computations, we need to calculate the wave number vector $\mathbf{k}$, given the direction of the ray tangent vector $\mathbf{t}$. This is done by solving the system of equations

$$\omega = \sigma + \mathbf{k} \cdot \mathbf{u}$$

$$(\mathbf{c}_g + \mathbf{u}) \times \mathbf{t} = \mathbf{0}$$

which is preferably rewritten in scalar form:

$$ku \cos (\theta - \varphi) + \sigma - \omega = 0 \tag{14}$$

$$c_g \sin (\theta - \alpha) + u \sin (\varphi - \alpha) = 0 \tag{15}$$

where $\varphi$ is the direction of the current $\mathbf{u}$ and $\alpha$ is the direction of the ray tangent vector. These equations are solved with respect to $k$ and $\theta$ using Newton's iterative method, making use of (6).

Now, assume that at some point along the ray $\mathbf{c}_g \cdot (\mathbf{c}_g + \mathbf{u})$ becomes zero. At this point the Jacobian $J(f, \theta)$ also becomes zero, and the directional spectrum density becomes infinite. This is physically acceptable, as the wave energy obtained by integration of $S(f, \theta)$ may still be finite. It is most probable, though, that at this point the waves are close to breaking, and

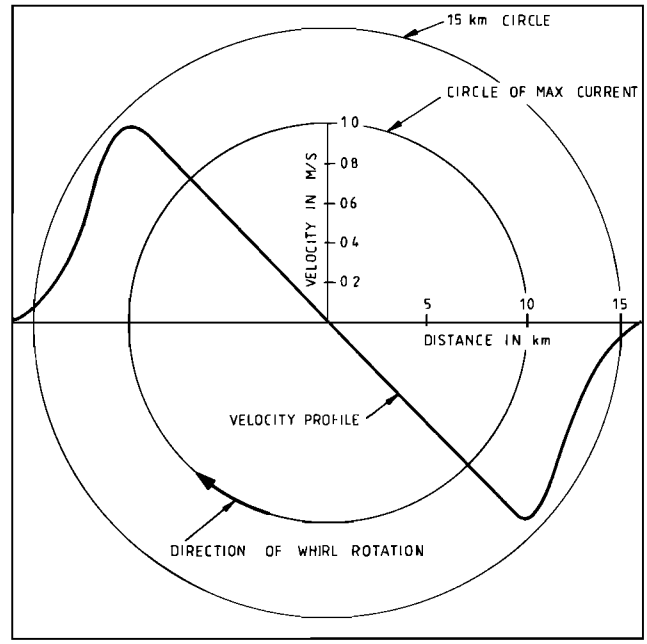


Fig. 1. Circular current whirl model and radial profile of tangential velocity.

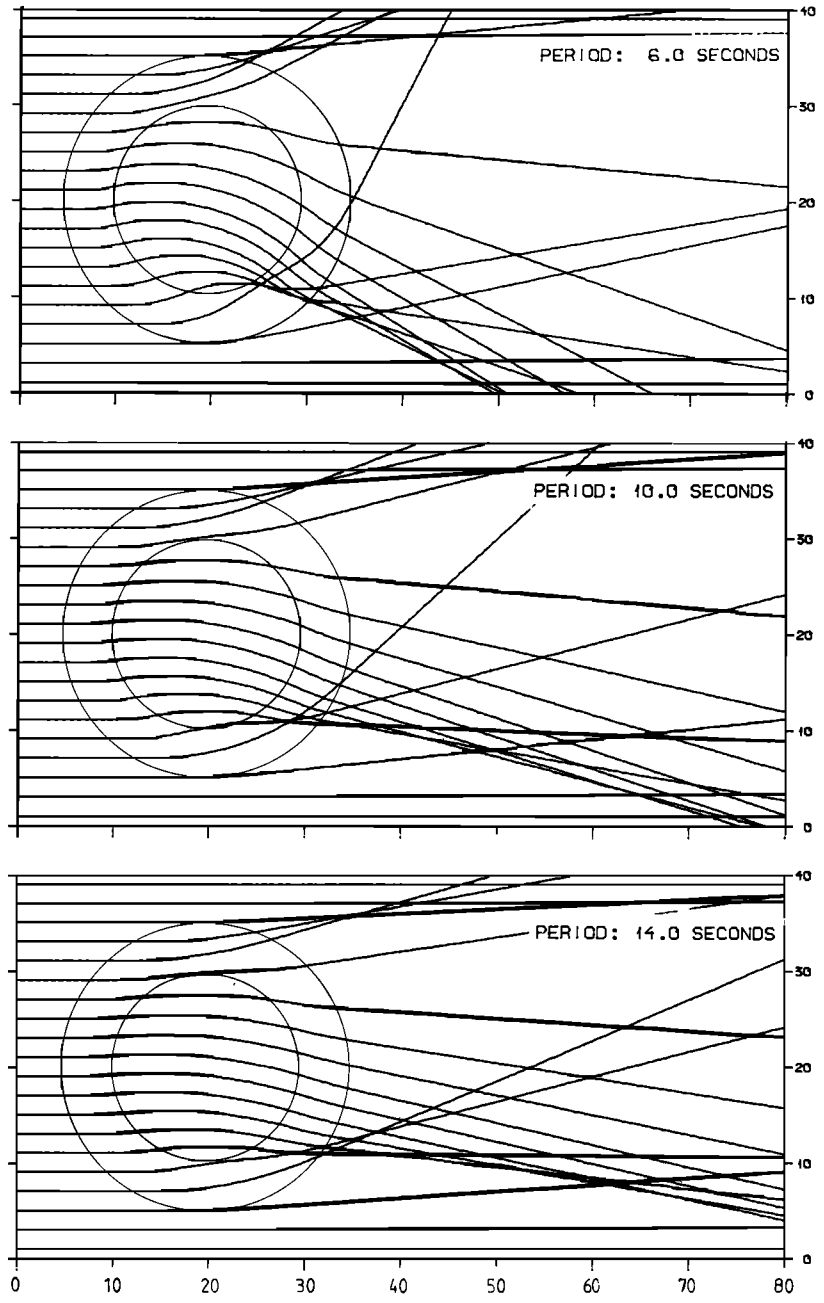


Fig. 2. Refraction diagrams for waves of period 6.0 s, 10.0 s, and 14.0 s.

the use of linear wave theory is questionable. In practice, therefore, the ray calculations are continued only as long as $\mathbf{c}_g \cdot (\mathbf{c}_g + \mathbf{u}) > 0$.

## CURRENT WHIRL MODEL

The occurrence of whirls in the Norwegian coastal current is most effectively inferred from satellite thermal images and field measurements of current velocity and sea temperature as shown by *McClimans and Nilsen* [1983]. The current within such whirls may be strong, and current speeds in excess of 1.5 m/s have been measured.

The study of whirls in the Norwegian coastal current has received much attention during the past few years. It is now well established that the occurrence of large current whirls is related to strong outflows of brackish water from the Skagerrak. As the brackish water flows northward along the coast of Norway, unstable waves or eddies, which can evolve into cyclonic or anticyclonic whirls, are formed along the current front.

The current whirl model we have chosen here is a highly idealized circular whirl. The tangential current velocity increases linearly from zero at the center of the whirl according to

$$u(r) = u_1(r/r_1) \qquad r \le r_1 < r_0$$

until the current speed is close to its maximum at $r = r_0$. Further away from the whirl center the current follows a

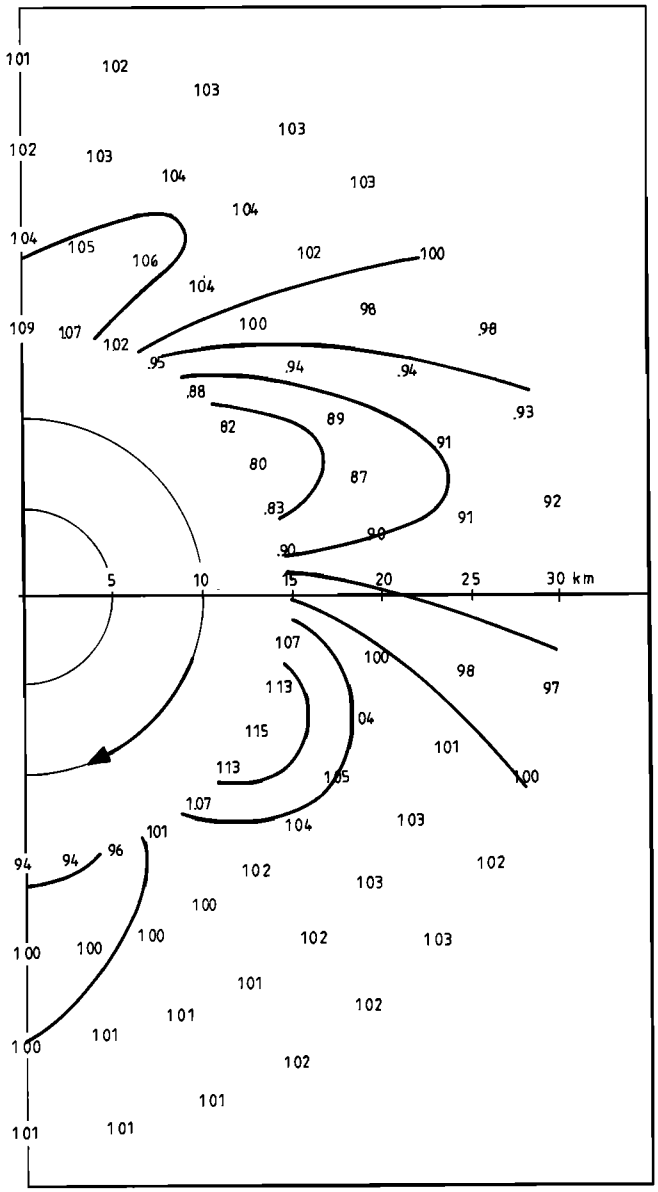


Fig. 3. Computed wave height coefficients for points outside the whirl for input spectral peak period of 10.0 s.

Gaussian profile,

$$u(r) = u_{max} \exp \{-[(r - r_0)/br_0]^2\} \qquad r > r_1$$

Continuity of $u$ and its derivative at $r = r_1$ requires that

$$r_1/r_0 = [1 + (1 - 2b^2)^{1/2}]/2 \tag{16}$$

$$u_1/u_{max} = \exp \{-[(r_1 - r_0)/br_0]^2\} \tag{17}$$

In the numerical computations we have chosen $u_{max} = 1.0$ m/s, $r_0 = 10$ km, and $b = 0.3$. The resulting model, shown in Figure 1, is considered to be fairly representative for the anticyclonic whirls occurring in the Norwegian coastal current.

For the numerical calculations we have chosen an 80 km × 40 km rectangular grid with triangular elements. The grid spacing is 800 m in both $x$ and $y$ directions. The water depth is set constant and equal to 200 m.

When computing the ray paths, we assume that the ray curvature is constant within each triangle. The wave parameters necessary for the computation of ray curvature are determined at triangle sides only.

In tests of ray computations, using unidirectional velocity profiles for which the wave directions can be determined analytically, the errors in computed wave directions were found to be within 0.1°. This is similar to the errors reported by *Treloar* [1986].

## Input Spectrum Model

The input offshore directional wave spectrum model $S(f, \theta)$ is written in the form

$$S(f, \theta) = S(f)D(f, \theta) \tag{18}$$

where $S(f)$ is the frequency spectrum and $D(f, \theta)$ is the directional distribution function described below. The directional distribution of wave energy is obtained by integration of $D(f, \theta)$ over the frequency range.

The frequency spectrum chosen is a Joint North Sea Wave Project (JONSWAP) spectrum model,

$$S(f) = \alpha g^2 (2\pi)^{-4} f^{-5} \exp\left\{-\frac{5}{4}\left(\frac{f}{f_p}\right)^{-4} + \ln(\gamma) \exp\left[-\frac{(f - f_p)^2}{2\sigma^2 f_p^2}\right]\right\} \tag{19}$$

where

$$\sigma = 0.07 \qquad f < f_p$$

$$\sigma = 0.09 \qquad f > f_p$$

The JONSWAP spectrum is uniquely determined by three parameters: the Phillips constant $\alpha$, the peak enhancement factor $\gamma$, and the peak frequency $f_p$. In practice, $\alpha$ is replaced by the significant wave height $H_{mo}$ in the choice of model parameters.

The most widely used directional distribution functions are proportional to some power of cos $(\theta)$ or cos $(\theta/2)$. Here we have chosen a Gaussian directional distribution,

$$D(f, \theta) = [1/(2\pi)^{1/2}\sigma_0] \exp[-(\theta - \theta_m)^2/2\sigma_0^2] \tag{20}$$

where the two parameters are the mean wave direction $\theta_m$ and the circular standard deviation $\sigma_0$.

The mean wave direction is assumed to be constant over the whole frequency range. However, the circular standard deviation is taken to vary with frequency according to

$$\sigma_0/\sigma_{0p} = (f/f_p)^{-2.03} \qquad f < f_p$$

$$\sigma_0/\sigma_{0p} = (f/f_p)^{+1.04} \qquad f > f_p$$

This formula is in agreement with the empirical results for the corresponding cos $(\theta/2)$ distribution function presented by *Hasselmann et al.* [1980]. The directional spread at the peak $\sigma_{0p}$ is here chosen equal to 0.349, i.e., 20°.

In the spectral current refraction study reported here, rays have been computed for wave periods from 4.5 s to 18.0 s at 1.5-s intervals and for wave directions at 2.5° intervals over the full circle. This means that 1450 rays have been computed for each "inshore" point chosen for the detailed spectrum analysis.

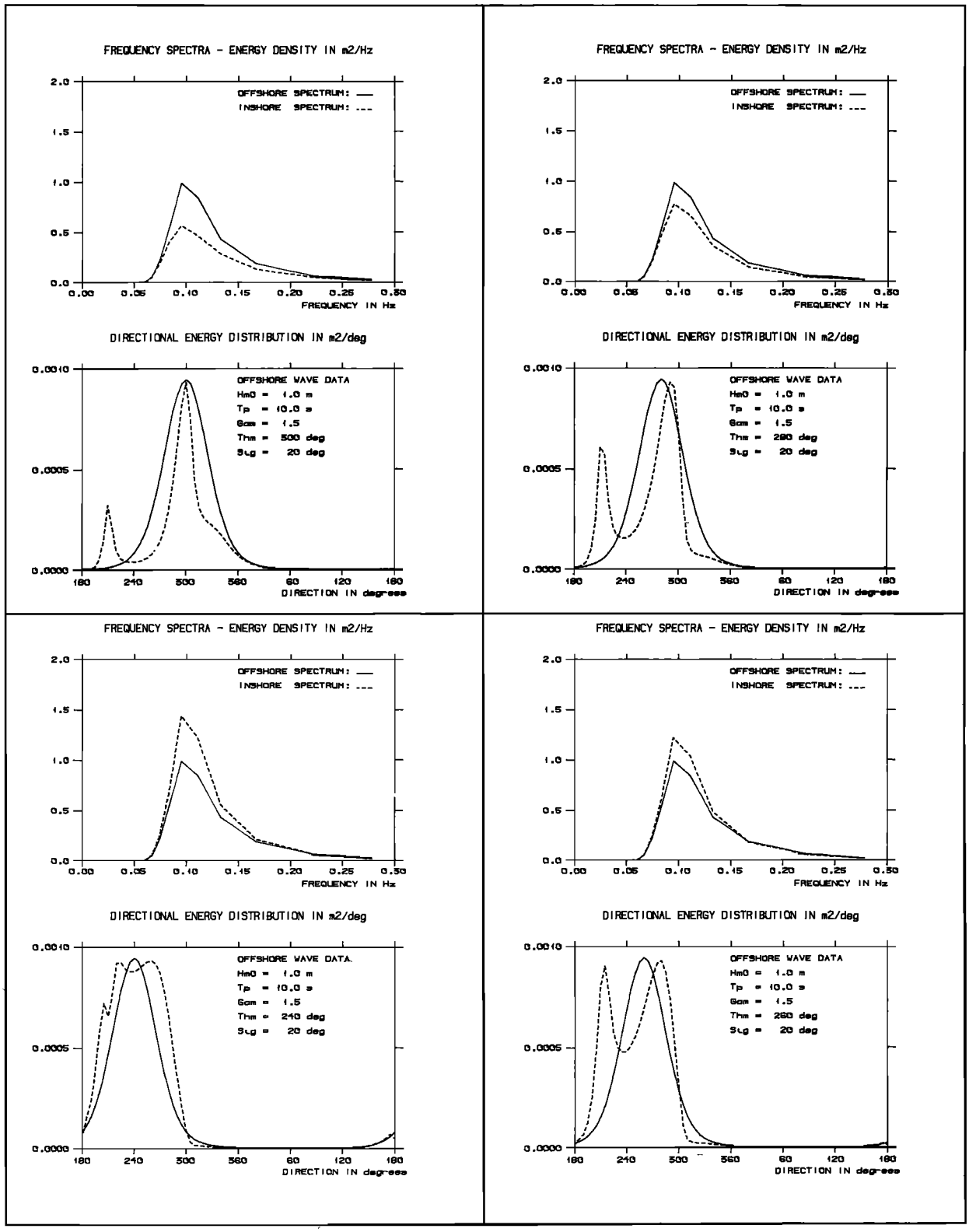


Fig. 4. Directional wave spectra for the point on the 15-km circle east of the whirl center for waves with mean wave directions Thm = 300°, 280°, 260°, and 240°.

## MODEL RESULTS

Results of wave refraction studies have traditionally been presented in terms of refraction diagrams. The rays which start out parallel from the offshore boundary, can be considered as streamlines of wave energy propagation. A convergence of rays indicates increasing concentration of wave energy and consequently increasing wave heights. Crossing rays indicate crossing seas and pyramidlike waves.

Figure 2 shows refraction diagrams for incoming waves with periods of 6, 10, and 14 s from the west. The distance between the rays is 2 km. Although the general refraction

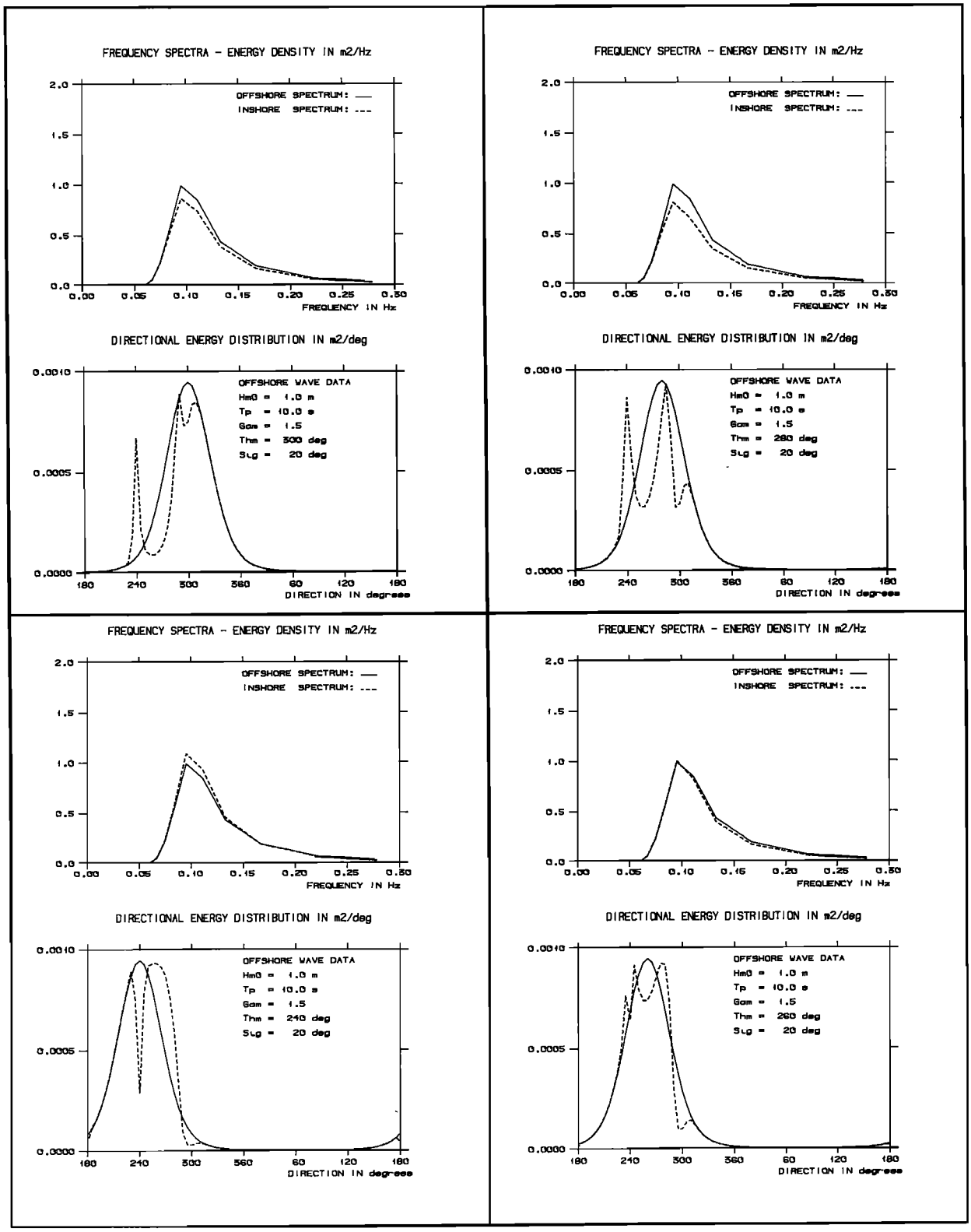


Fig. 5. Directional wave spectra for the point on the 25-km circle east of the whirl center for waves with mean wave directions Thm = 300°, 280°, 260°, and 240°.

pattern is the same, we see that current refraction affects the high-frequency waves more than it affects the low-frequency waves.

The refraction diagrams show two areas of crossing seas, one area of relatively strong focusing of wave energy to the southeast of the whirl center and one minor focusing area to the northeast. In between these areas we find an area of reduced energy concentration.

A more detailed description of how the current whirl affects the wave conditions, is obtained from spectral computations.

TABLE 1. Computed Wave Height Coefficients at the Point 15 km East of the Whirl Center

| Offshore Wave Direction, deg | Offshore Peak Period, s | | | | | | |
|---|---|---|---|---|---|---|---|
| | 16.7 | 14.3 | 12.5 | 11.1 | 10.0 | 9.1 | 8.3 |
| 180 | 0.95 | 0.94 | 0.94 | 0.94 | 0.94 | 0.94 | 0.94 |
| 200 | 0.96 | 0.96 | 0.96 | 0.96 | 0.96 | 0.96 | 0.98 |
| 220 | 1.06 | 1.06 | 1.06 | 1.07 | 1.07 | 1.08 | 1.08 |
| 240 | 1.13 | 1.14 | 1.14 | 1.15 | 1.15 | 1.15 | 1.14 |
| 260 | 1.06 | 1.07 | 1.07 | 1.07 | 1.07 | 1.06 | 1.05 |
| 280 | 0.93 | 0.92 | 0.91 | 0.91 | 0.90 | 0.89 | 0.89 |
| 300 | 0.86 | 0.84 | 0.83 | 0.82 | 0.80 | 0.79 | 0.79 |
| 320 | 0.92 | 0.91 | 0.90 | 0.89 | 0.88 | 0.87 | 0.86 |
| 340 | 1.02 | 1.02 | 1.02 | 1.02 | 1.02 | 1.03 | 1.03 |
| 360 | 1.06 | 1.07 | 1.07 | 1.08 | 1.09 | 1.10 | 1.10 |

TABLE 3. Computed Mean Wave Directions at the Point 15 km East of the Whirl Center

| Offshore Wave Direction, deg | Offshore Peak Period, s | | | | | | |
|---|---|---|---|---|---|---|---|
| | 16.7 | 14.3 | 12.5 | 11.1 | 10.0 | 9.1 | 8.3 |
| 180 | 177 | 177 | 177 | 177 | 177 | 178 | 178 |
| 200 | 200 | 201 | 202 | 203 | 204 | 205 | 206 |
| 220 | 224 | 225 | 226 | 227 | 228 | 229 | 230 |
| 240 | 240 | 240 | 240 | 241 | 241 | 242 | 243 |
| 260 | 255 | 254 | 253 | 253 | 252 | 252 | 252 |
| 280 | 275 | 274 | 272 | 271 | 269 | 268 | 267 |
| 300 | 299 | 298 | 298 | 297 | 295 | 294 | 293 |
| 320 | 322 | 322 | 322 | 322 | 321 | 321 | 321 |
| 340 | 339 | 339 | 338 | 338 | 338 | 337 | 337 |
| 360 | 356 | 355 | 355 | 354 | 354 | 353 | 353 |

Figure 3 shows computed wave height coefficients in the area to the east of the whirl resulting from incoming waves from the west with a spectral peak period $T_p$ of 10.0 s. The wave height coefficients are defined as local significant wave height divided by offshore significant wave height. The figure gives a quantitative description of the general refraction pattern seen in the refraction diagrams.

Directional spectral for two points on the 15 and 25 km circles east of the whirl centre, is presented in Figures 4 and 5. In the figures the whole lines represent the input offshore spectra, while the broken lines represent the computed inshore spectra. The only parameter varied in these spectral presentations, is the mean wave direction $\theta_m$ (Thm in Figures 4 and 5). However, because of the symmetry of the problem, these spectra can also be seen as the spectra resulting from incoming waves from the west at points on the 15- and 25-km circles in the direction $360° - \theta_m$ as viewed from the whirl center. The wave direction is here the direction from which the waves come and is measured in degrees clockwise from north.

The point of minimum wave height on the 15-km circle is in direction 60° (see Figure 3). The directional spectrum for this point which corresponds to $\theta_m = 300°$ is shown in Figure 4. We see that the directional distribution is bimodal with a very narrow main lobe. Consequently, the sea here has a well-defined dominant wave direction and some low-energy waves propagating in the direction normal to the main wave direction.

Moving southward along the 15-km circle, that is, considering spectra for decreasing values of $\theta_m$, we see that the energy in the directional side lobe grows until we reach the point of maximum wave height for $\theta_m = 240°$. The directional distribution of wave energy has become unimodal, but very broad. The result is a confused sea with pyramidlike waves. The same general pattern is repeated along the 25-km circle, but the refraction effects are seen to be less pronounced (see Figure 5).

Computations have also been made for other input spectral peak wave periods. Results from these calculations are presented in Tables 1, 2, and 3. The general impression is that the computed wave parameters are relatively insensitive to the choice of peak wave period.

A generalization of the results presented is achieved by introducing nondimensional variables. Let $L$, $T$, and $U$ be characteristic length, time, and current velocity scales. The deepwater wave refraction problem considered can then be characterized by two nondimensional numbers $\alpha$ and $\beta$,

$$\alpha = gT^2/L \qquad \beta = UT/L$$

In order to keep $\alpha$ and $\beta$ constant, we see that if $T$ is doubled, $L$ has to be increased by a factor of 4 and $U$ by a factor of 2.

TABLE 2. Computed Mean Wave Periods at the Point 15 km East of the Whirl Center

| Offshore Wave Direction, deg | Offshore Peak Period, s | | | | | | |
|---|---|---|---|---|---|---|---|
| | 16.7 | 14.3 | 12.5 | 11.1 | 10.0 | 9.1 | 8.3 |
| 180 | 12.4 | 11.0 | 9.7 | 8.6 | 7.8 | 7.1 | 6.5 |
| 200 | 12.3 | 11.0 | 9.7 | 8.6 | 7.8 | 7.1 | 6.5 |
| 220 | 12.6 | 11.2 | 9.9 | 8.8 | 8.0 | 7.3 | 6.7 |
| 240 | 12.9 | 11.4 | 10.1 | 9.0 | 8.2 | 7.5 | 6.9 |
| 260 | 12.7 | 11.3 | 10.0 | 9.0 | 8.1 | 7.4 | 6.8 |
| 280 | 12.3 | 11.0 | 9.8 | 8.7 | 7.9 | 7.2 | 6.7 |
| 300 | 12.1 | 10.8 | 9.6 | 8.5 | 7.7 | 7.0 | 6.5 |
| 320 | 12.4 | 11.0 | 9.7 | 8.7 | 7.8 | 7.1 | 6.6 |
| 340 | 12.7 | 11.2 | 9.9 | 8.9 | 8.0 | 7.3 | 6.7 |
| 360 | 12.6 | 11.2 | 9.9 | 8.9 | 8.0 | 7.3 | 6.8 |

## DISCUSSION

When waves encounter an opposing current, the high-frequency spectral density can increase until the equilibrium range is reached and the waves start to break. Therefore the relative change in wave height within the current whirl generally depends on the absolute energy of the incoming waves. This argument also applies to points outside the current whirl, but to a lesser degree.

From the above it is clear that the results of the wave height computations for points outside the current presented in Figure 3 are not independent of the input wave spectra. For higher sea states this means that the computed high-frequency spectral density is too large. However, as long as the input wave spectra represent moderate sea states, the accuracy of the computed wave height coefficients is not much affected, as the spectral density in the high frequency region is relatively low.

In wave refraction studies where accurate wave height estimates are needed, this problem can be overcome by introduc-

ing *Phillips'* [1985] equilibrium wave number spectrum form $\beta(\cos\theta)^p(u_*/c)k^{-4}$, where $\beta \approx 0.01$, $p \approx \frac{1}{2}$, and $u_*$ is the friction velocity. This form is applied to the highest value of the wave number $k$ attained along the ray. The same procedure is described by *Phillips* [1977, pp. 77–78] for the case of unidirectional waves opposing a unidirectional current.

The results of the wave refraction computations indicate that the changes in wave height on the lee side of the whirl are within $\pm 20\%$, which may not seem important as regards the navigational conditions in this area. However, the changes in directional properties are considerable, varying from nearly unidirectional waves to chaotic crossing seas with pyramidlike waves. Such waves are likely to create difficult navigational conditions for passing ships.

## CONCLUSIONS

A computer model for the computation of refraction of directional wave spectra is described. The model is applied to a circular current whirl typical for the whirls appearing in the Norwegian coastal current. Wave heights are computed for points outside the whirl. The relative changes in wave heights are found to be within $\pm 20\%$ as compared with the wave height of the incoming waves. The computations reveal two areas of crossing seas on the lee side of the whirl. Between these areas is an area of reduced wave heights and nearly unidirectional waves.

The results presented are fairly general, but they apply only to nonbreaking waves. It is shown how the range of applicability of the computer model can be extended by introducing a limiting equilibrium spectrum form.

The wave refraction model can be used to produce detailed directional wave spectrum information based on realistic input wave data. It is therefore useful in localizing areas of crossing seas hazardous to passing ships.

*Acknowledgment.* This work was supported by the Royal Norwegian Council for Scientific and Industrial Research.

## REFERENCES

Abernethy, C. L., and G. Gilbert, Refraction of wave spectra, *Rep. INT 117*, Hydraul. Res. Sta., Wallingford, England, 1975.

Bretherton, F. P., and C. J. R. Garrett, Wavetrains in inhomogeneous media, *Proc. R. Soc. London, Ser. A, 302*, 529–554, 1968.

Brink-Kjœr, O., Depth-current refraction of wave spectra, paper presented at the Symposium on Description and Modelling of Directional Seas, Technical University of Denmark, Copenhagen, June 18–20, 1984.

Hasselmann, D. E., M. Dunckel, and J. A. Ewing, Directional wave spectra observed during JONSWAP 1973, *J. Phys. Oceanogr., 10*, 1264–1280, 1980.

Longuet-Higgins, M. S., On the transformation of a continuous spectrum by refraction, *Proc. Cambridge Philos. Soc., 53*, 226–229, 1957.

Mapp, G. R., C. S. Welch, and J. C. Munday, Wave refraction by warm core rings, *J. Geophys. Res., 90*(C4), 7153–7162, 1985.

Mathiesen, M., Current-depth refraction of directional wave spectra, paper presented at the Symposium on Description and Modelling of Directional Seas, Technical University of Denmark, Copenhagen, June 18–20, 1984.

McClimans, T. A., and J. Nilsen, Whirls in the Norwegian coastal current, in *Proceedings of a NATO Advanced Research Institute in Coastal Oceanography, Os, Norway, June 6–11 1982*, edited by H. Gade, A. Edwards, and H. Svendsen, Plenum, New York, 1983.

Phillips, O. M., *The Dynamics of the Upper Ocean*, 2nd ed., 336, pp., Cambridge University Press, New York, 1977.

Phillips, O. M., Spectral and statistical properties of the equilibrium range in wind-generated gravity waves, *J. Fluid Mech., 156*, 505–531, 1985.

Tayfun, M. A., R. A. Dalrymple,, and C. Y. Yang, Random wave-current interactions in water of varying depth, *Ocean Eng., 3*, 403–420, 1976.

Treloar, P. D., Spectral wave refraction under the influence of depth and current, *Coastal Eng., 9*, 439–452, 1986.

M. Mathiesen, Norsk Hydroteknisk Laboratorium, N-7034 Trondheim NTH, Norway.

(Received September 27, 1986;
accepted November 17, 1986.)